CHARACTERIZATION OF THE ACYL-COA BINDING DOMAIN CONTAINING 3 PROTEIN

A THESIS SUBMITTED TO THE GRADUATE DIVISION OF THE
UNIVERSITY OF HAWAII IN PARTIAL FULFILLMENT
OF THE REQUIREMENTS FOR THE DEGREE OF

MASTER OF SCIENCE

IN

MICROBIOLOGY

MAY 2006

By
Zengqiu Li

Thesis Committee:

Helen Turner, Chairperson

Paul Patek

Tung Hoang

We certify that we have read this thesis and that, in our opinion, it is satisfactory in scope and quality as a thesis for the degree of Master of Science in Microbiology.

THESIS COMMITTEE

Chairperson

ACKNOWLEDGEMENTS

I would like to thank the following people for their valuable contributions to this project:

My parents for their support of my overseas life.

Dr. Michael Dunn for helping me get to the University of Hawaii and as a result into Dr. Helen Turner's lab.

Dr. Alexander Stokes for sharing his knowledge and enthusiastic technical assistance.

Mr. Clay Wakano, Dr. Kimberly Del Carmen, Mrs. Lori Shimoda, and Mrs. Linden Doescher for sharing their knowledge and their time.

The other members of The Queen's Center for Biomedical Research for their generous help.

The members of my thesis committee, Dr. Paul Patek and Dr. Tung Hoang, for their time and flexibility.

Special and the greatest thanks go to Dr. Helen Turner. Without her guidance and patience, I would never have been able to have this project done.

TABLE OF CONTENTS

LIST OF ABBREVIATIONS

Amp:	ampicillin
AKAP:	A kinase anchoring protein
Bp:	base pair
cDNA:	complementary DNA
CIP:	calf intestinal phosphatase
CNS:	central nervous system
DNA:	deoxyribonucleic acid
dsDNA:	double strand DNA
E. coli:	*Escherichia coli*
ECL:	enhanced chemi-luminescence
EDTA:	ethylenediamine tetra-acetic acid
g :	gravity = rcf (relative centrifugal force)
GST:	glutathione-S-transferase
HEPES:	N-2-hydroxyethylpiperazine-N'-2-ethanesulfonic acid
IMAC:	immunobilized metal affinity chromatography
IPTG:	isopropyl-2-D-thiogalactopyranoside
kDa:	kiloDalton
LB:	Luria-Bertani
min:	minute
MOPS:	4-Morpholinepropanesulphonic acid
mRNA:	messenger RNA
PAGE:	polyacrylamide gel electrophoresis
PBS:	phosphate-buffered saline
PCR:	polymerase chain reaction
PKA:	protein kinase A
PKC:	protein kinase C
PKD:	protein kinase D
PKG:	protein kinase G

PKN:	protein Kinase N
RE:	Restriction endonuclease, restriction enzyme
rpm:	rotations per minute
RNA:	ribonucleic acid
RT-PCR:	reverse transcription polymerase chain reaction
SDS:	sodium dodecyl sulphate
TAE:	tris/acetate/EDTA buffer
Tris:	tris(hydroxymethyl)amino-methane
TRPV1:	transient receptor potential cation channel, subfamily V, member 1
TRPV2:	transient receptor potential cation channel, subfamily V, member 2
VR-1:	Vanilloid Receptor-1
v/v:	volume/volume
WB:	Western Blot
v/v:	weight/volume
w/w:	weight/weight
Y2H:	Yeast two-hybrid

LIST OF FIGURES

ABSTRACT

The cAMP dependent protein kinase, PKA, is of great importance for cells to transduce extra- and intra-cellular signals. Recent studies have found that signal transduction through PKA is coordinated by a group of scaffold proteins called A-Kinase Anchoring Proteins. These AKAPs, together with PKA and its substrates, form a dynamic assembly that tightly controls the location and timing of signal transduction events, which in turn regulates various cellular activities including ion channel modulation, cell growth, cell differentiation and cytokinesis. Previous research in Dr. Turner's lab has found that TRPV ion channels recruit PKA through Acyl-CoA Binding Domain containing 3 protein (ACBD3) to transduce physiological stimuli in mast cells and sensory neurons. Other studies have indicated a similar role for ACBD3 during PKA-mediated steroid formation. Hence, we hypothesize that ACBD3 may function as an AKAP recruiting PKA to multiple novel targets, in addition to ion channels such as the TRPVs. The project presented in this paper aimed at production of purified ACBD3 protein, for use as an affinity matrix to purify novel targets of ACBD3. The human ACBD3 cDNA was subcloned into the pTrcHisB vector with a conferred epitope tag comprising six sequential Histidine residues. Then the construct was transformed into the BL21 *E.coli* strain to express the protein in an inducible manner. Finally, we used Immunobilized Metal Affinity Chromatography (IMAC) technique to purify the fusion protein. With the purified protein, we confirmed the strong PKA binding ability of ACBD3, which is consistent with our hypothesis. We also demonstrated a wide expression profile of ACBD3 in different tissues, suggesting that ACBD3 is likely to function outside the CNS and hence is likely to interact with proteins other than TRPVs.

Chapter 1

Introduction

1.1. The PKA signaling pathway.

The cAMP dependent kinase A (PKA) pathway is a ubiquitous signaling pathway in eukaryotic cells. It regulates a great variety of cellular activities [1, 2]. Critical roles of PKA in signal transduction processes are illustrated by the diversity of its substrates. Hundreds of PKA substrates so far have been found. These substrates are involved in a wide range of cellular functions, and include ion channels, transcription factors and cytoskeletal proteins [3-5].

The signaling transduction pathway that activates PKA starts from G Protein Coupled Receptors (GPCR) in response to hormone, growth factor, or neurontransmitters. These extra-cellular ligands bind to GPCRs in the plasma membrane causing generation of cAMP by adenylyl cyclases, which are under the regulation of heterotrimeric G proteins. The signaling system downstream of adenylyl cyclases employ PKA, in most cases, and other protein kinases that responsed to change in cAMP concentration [6].

PKA is a heterotetramer, with two Regulatory (R) and two Catalytic (C) subunits. There are two isotypes of PKA due to the expression of isoforms of the R subunit, RI and RII. In the inactive state, R units bind to C units of PKA. Once an elevation in cAMP levels is generated, cAMP molecules occupy their binding sites on the R units leading to a

conformational change in the R units. This causes the C subunits to be released from the inactive PKA assembly [1]. Without the inhibitory presence of the R subunits, the C subunits are catalytically active. Active PKA are then able to phosphorylate serine and threonine residues on their specific substrates using the catalytically active C subunits [7].

1.2 Signal transduction and protein-protein interactions of the PKA enzyme.

For cells to differentiate or to divide, to attach or to move, to survive or to die, these decisions must be accurate and well coordinated in space and in time. The action that a cell needs to take is dictated both by factors external to the cell and by internal signals. Signal transduction pathways represent the mechanisms by which cells carry out these decisions. Protein-protein interactions are the key elements of the signaling machinery.

Since the completion of the human genome sequence, the number of recognized signaling proteins has greatly increased and the models of these pathways are highly complicated. Although many signaling pathways seem complex when viewed as a whole, at a closer sight these pathways often can be described in terms of series of simple interactions of one protein with another [8]. Indeed, these interactions are so fundamental that they form the basis of all signal transduction mechanisms. Therefore, focusing on protein-protein interactions is one of the basic routes to study signal transduction events [7, 9].

1.3 A Kinase Anchoring Proteins (AKAP) and their regulation of PKA.

Numerous studies have found that local cellular signaling events are largely due to protein-protein interactions that form macromolecular complexes. Scaffolds, adapters, and

inhibitors often form the basic protein framework of signaling transduction events [10]. For example, it is these complexes that achieve temporal and spacial targeting of signaling proteins.

Central to these signaling complexes are thought to be scaffold proteins, of which the AKAPs are well studied examples. For example, AKAPs are scaffold proteins that recruit PKA to its substrates [11-13]. It is notable that the family of AKAPs is classified by their functional similarity of being able to bind to PKA. AKAP family members thereby share few common structural properties [14]. The first identified AKAP was microtubule associated protein 2 (MAP2) because it was co-purified with PKA RII subunits [15].

It is now clear that most of AKAPs bind to the PKA RII subunit, whereas a few of them exhibit dual specificity, binding to both RI and RII [16-20]. AKAPs are also able to bind to PKC, PKD, the Rho-activated kinase PKN protein, phosphatases and other downstream targets and this indicates a wide range of binding specificity for these scaffold proteins [11, 21]. Binding to both kinases and protein phosphatases provides one of the AKAPs most valuable features: precise regulation of the phosphorylation status of substrates, with bidirectional control of phosphate transfer.

AKAPs can bind to the PKA R subunit after SDS-PAGE and electrotransfer to nitrocellulose membranes. Although AKAPs are unlikely to share primary sequence homology, the R subunit binding domains contain a conserved motif, which is an amphipathic helix structure [17, 18, 22]. Peptides generated from this structure of Human Thyroid AKAP (HT31) specifically disrupts the interaction between R subunit of PKA and AKAP. Thereby, the HT31 anchoring inhibitor has been widely used to characterize the

functional role of PKA anchoring in intact cells.

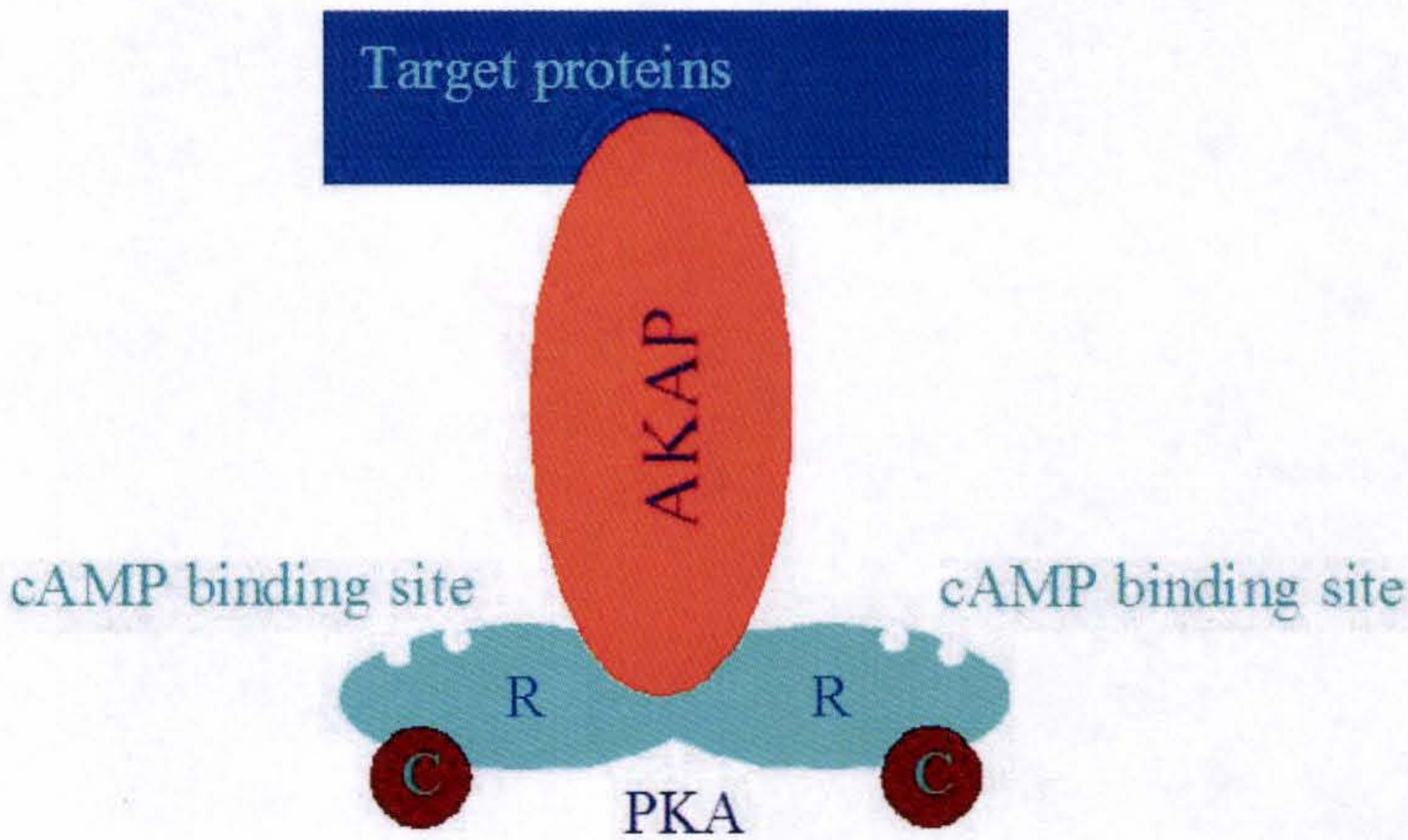

Figure 1.3.1: Schematics of the AKAP-PKA complex. PKA phosphorylation on target proteins is regulated by AKAP. In order to provide spatial and temporal control of the phosphorylation of target proteins, the AKAP is required to bind to both target proteins and PKA R subunits. PKA C subunits are binding to R subunits in the resting state. When cAMP binding occurs, C subunits detach from R subunits, move to target proteins and transfer phosphate to them.

1.4 ACBD3 and its interaction with PKA and ion channels, including the TRPVs.

Acyl Co-A Binding Domain containing 3 (ACBD3) is a 528 amino acid protein that was previously known as "Peripheral-type benzodiazepine receptor and PKA Associated Protein7" (PAP7) [23, 24]. By comparison with AKAP, the function of ACBD3 in transducing the cAMP signal is similar to that of human AKAPs in various signaling pathways [25]. The fact that ACBD3 was isolated using PKA-RI as bait from human

lymphocyte library in a yeast two hybrid experiment is one of the lines of evidence that the idea supporting that ACBD3 is a member of AKAP family [23]. Dual-AKAP1 (D-AKAP1) is a member of the AKAP family that can interact with both RI and RII PKA subunits [16]. A comparison of 30 amino acids of one targeting motif of D-AKAP1 to ACBD3 shows a high level of homology, also suggesting that ACBD3 may be part of the AKAP family.

1.4.1 Structural and sequence properties of ACBD3.

ACBD3 is a 528 amino acid protein with a calculated molecular mass of about 61kDa (predicted by MacVector). By using a Swiss-Prosite profile scan, we found that ACBD3 contains an Acyl-CoA enzyme binding domain (a.a.104-122) and a GOLD domain (a.a.384-526). The GOLD (for Golgi dynamics) domain is a protein module found in several eukaryotic Golgi and lipid-traffic proteins. In these proteins, the GOLD domain co-exists with lipid-, sterol- or fatty acid binding domains, and acyl CoA-binding domains, suggesting that these proteins are likely to interact with membranes. The GOLD domain is predicted to mediate diverse protein-protein interactions. These predictions suggest the possibility that ACBD3 may play a role in regulation of various membrane proteins including transporters and ion channels through their protein-protein interactions. Figure 1.4.1 shows the schematic picture of ACBD3 protein with ACBP and GOLD domains.

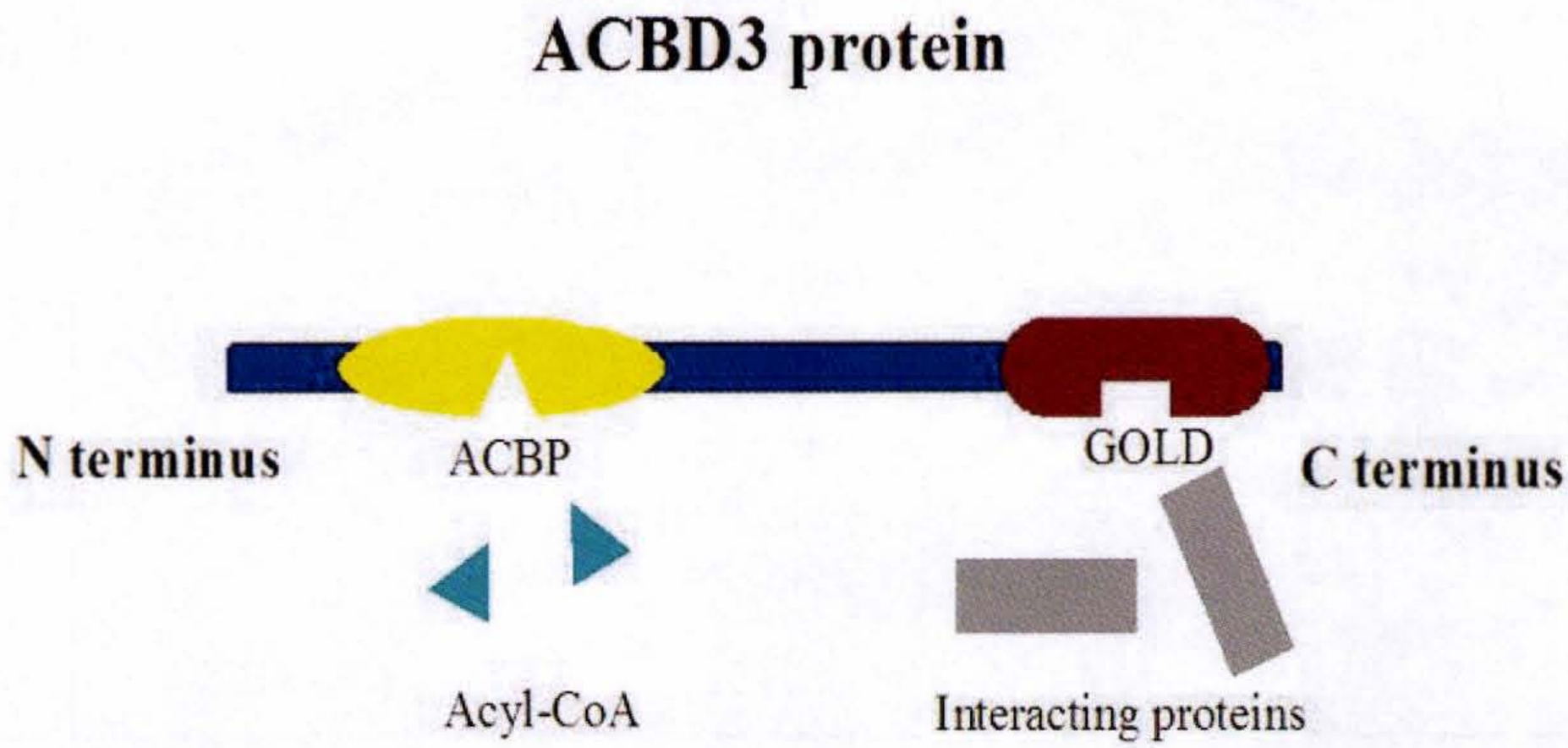

Figure 1.4.1 Schematic of the ACBD3 protein.

The full length of ACBD3 is 528 amino acids. There are only two functional domains predicted according to Swiss-Prosite database. The Acyl-CoA Binding domain is located at positions 104-122. The GOLD (for golgi dynamic) domain is located at positions 384-526 , which are very close to the C terminus.

Moreover, ACBD3 contains sequence regions that are rich in proline (a.a.21-60), glutamic acid (a.a.182-240), arginine (a.a.196-238), and glutamine (a.a.241-308). We also found the ACBD3 has five potential PKC phosphorylation sites (a.a.47-49, 178-180, 320-322, 345-347, and 404-406); eight potential casein kinase II phosphorylation sites (a.a.105-108, 128-131, 153-156, 340-343, 345-348, 409-412, 450-453 and 451-454); two potential tyrosine kinase phosphorylation sites (a.a.278-285 and 485-492); two potential N-terminal glycosylation sites (a.a.151-154 and 324-327) and one potential N-terminal myristoylation site. It is notable that there is no PKA phosphorylation site predicted on the ACBD3 protein, which apparently excludes the possibility of being phosphorylated by PKA when PKA-ACBD3 complex is present.

Our laboratory has previously generated data suggesting that ACBD3 may be an AKAP

for the TRPV ion channels. These channels are physical sensors involved in regulation of the Central Nervous System (CNS) and the immune system [26]. Therefore, it is of interest to understand their regulatory signaling. TRPV1 is a heat-transducing and capsaicin-sensitive vanilloid receptor, which was previously called VR-1 [27, 28]. PKA phosphorylation alters the activity of the channel, and PKA phosphorylation of TRPV1 has been shown to be mediated by AKAP using the HT31 inhibitor peptide [29]. Yeast two hybrid results using TRPV2, another member in TRPV family with a higher heat threshold than TRPV1, as bait, showed that ACBD3 may also mediate the interaction between PKA and TRPV2 [30]. All these data suggest that ACBD3 may play a critical role in phosphorylation of TRPV channels and potentiating the cellular responses to heat and other physical and chemical stimuli. We are also interested in establishing novel protein targets for the AKAP activity of ACBD3.

1.5 Use of His-tagged fusion proteins in the biochemical study of protein-protein interactions.

The overall goal of our work on ACBD3 is to identify proteins that mediate ACBD3 signaling. As mentioned in Chapter 1.2, most signaling pathways depend upon protein-protein interactions. We therefore need to generate a tool which is able to bind to potential partners for ACBD3 for the study of protein-protein interaction that can then be detected using conventional biochemical techniques.

Tagged fusion proteins, or similarly "recombinant" fusion proteins are used extensively in pull-down assays, affinity purification, and Far-Western analysis. These techniques have been used commonly in the study of protein-protein interactions for proteins that represent

drug targets. Common protein fusion systems include: a polyhistidine tag (His-tag) fusion; glutathione-S-transferase (GST) fusion; maltose binding protein (MBP) fusion [31-33]. Although His-tagged and GST (GST tag is a 26kDa protein) fusion proteins are the most commonly used systems, the His-tag fusion system is preferable to the GST fusion system because the 6 X histidine tag is smaller, and is thus less likely to interfere with protein functionary folding and function.

The flexibility of His-tagged fusion protein affinity purification permits its application to a wide range of biological questions. Affinity purification using His-tagged fusion proteins allow a large scale screen of a cytosolic extract with a novel protein bait to identify new interactions, as well as to identify specific regions of proteins that mediate these interactions. Moreover, these approaches can be initiated prior to the availability of antibodies to the protein of interest, or when antibodies to the protein have been found to interfere with its protein-protein interaction. However, it is necessary to note that these methods characterize *in vitro* interactions, which should subsequently be verified *in vivo* by other means such as immunoprecipitation.

His-tag fusion proteins incorporate a polyhistidine stretch that can be purified by its high-affinity binding to metal ions such as Ni^{2+}. This system has the advantage that the fusion protein can be denatured during the purification while the His-tag is still competent to bind to metal ions, allowing a denatured fusion protein to be affinity-purified. This is a distinct advantage for insoluble proteins. It is preferable however, to optimize purification conditions so that native protein structure is conserved. Many of these fusion protein vectors are available for bacterial, insect, and mammalian expression systems.

His-tagged fusion protein affinity purification is able to screen unknown proteins in solution through their interactions with His-tagged probe protein and allows isolation of the complex by collection of the interacting proteins through the binding of His-tag to nickel ion coupled beads. Western analysis can be then used with membranes generated by transfer after SDS-PAGE, allowing detection of and information about the size, of interacting proteins.

1.6 Hypothesis and goals.

Based on the previous results from our laboratory, the hypothesis of this study is that ACBD3 is a PKA regulator and may function as an AKAP recruiting PKA to substrates that include ion channels and other as yet undescribed proteins. Our strategy is to use purified His-tagged ACBD3 as a probe to: (1) confirm that ACBD3 binds to PKA; (2) generate a tool that can be used to affinity purify and identify novel ACBD3 interacting proteins.

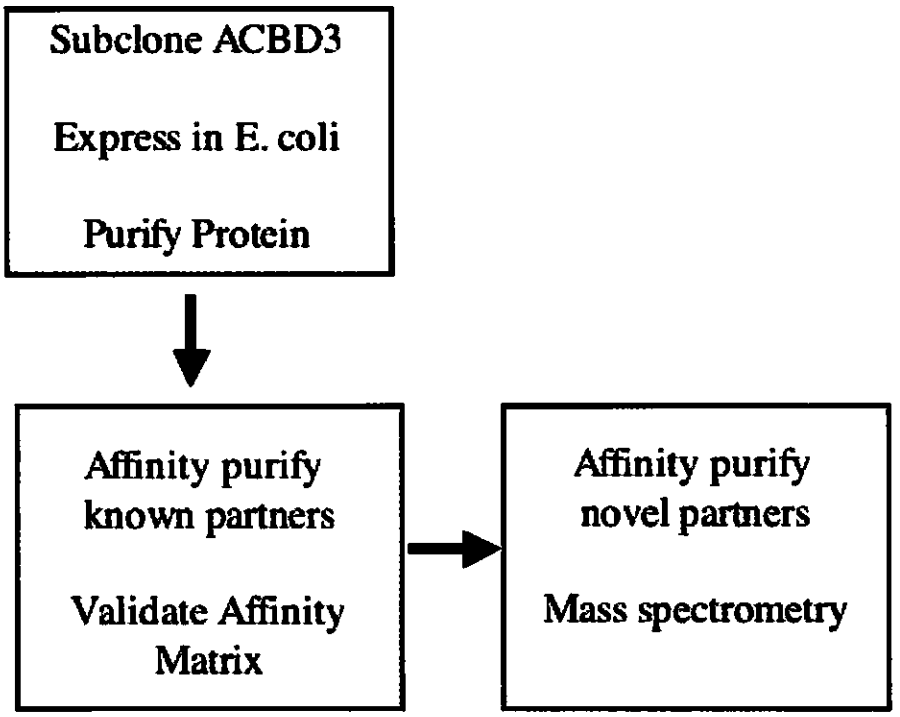

Figure 1.6.1 Flow chart of the proposed project

CHAPTER TWO

Methods and Materials

2.1. PCR.

A sense primer, AGCAGCGAATTCGATGGCGGCGGTGCTGAACGCAGAG, and an anti-sense primer, GCTGCTGCGGCCGCTTATCTAGTATAATAGACTCTGTAGTAGAC TGATTTTGACCGG, were designed based on the human ACBD3 cDNA sequence according to the NCBI database (accession ID: BC060792). The oligonucleotides were obtained by purchase (Invitrogen, Carlsbad, CA.) and the cDNA template was purchased from Open Biosystems. *EcoRI* and *NotI* substrate sequences were introduced to the primers (underlined). Figure 2.1.1 shows the schematics of primers. PCR was performed for 35 cycles of denaturation (95°C, 30 seconds), annealing (63.2°C, 30 seconds), and extension (68°C, 1.5 minutes) using the AccuPrime™ *Pfx* SuperMix (Invitrogen, Carlsbad, CA). PCR product was first confirmed by agarose gel electrophoresis as an approximate 1.5 kb fragment, and then extracted from agarose gel using the QIAquick Gel Extraction Kit (Qiagen, Valencia, CA).

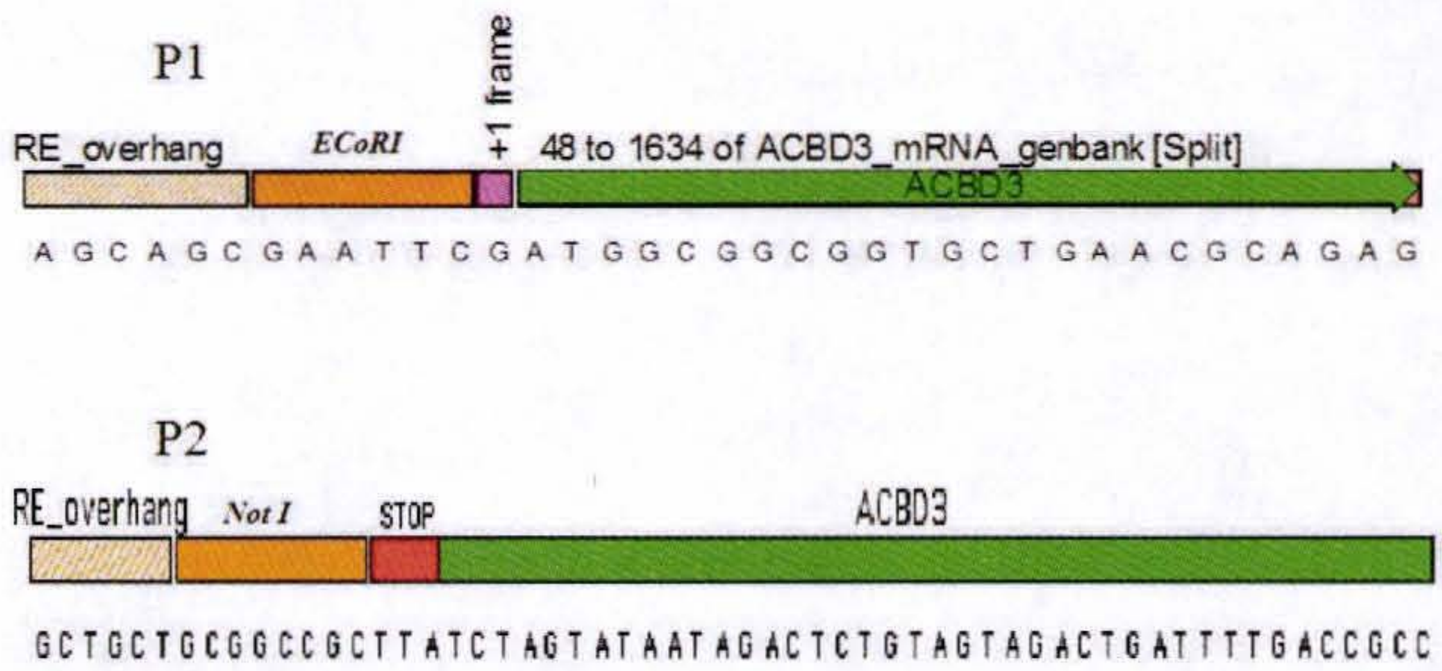

Figure 2.1.1 Sequence and schematic of PCR primers of ACBD3. Each primer contains a restriction enzyme overhang, restriction emzyme site and 5' and 3' end of ACBD3 cDNA, respectively. One extra base pair (G) is added upstream of the ATG translational start codon in order to prevent frame shift.

2.2 Gel electrophoresis of DNA.

The agarose gel electrophoresis used 1% agarose in TAE buffer (40mM Tris, 20mM Acetic acid, and 2mM EDTA pH 8.3). DNA samples were loaded in sample buffer containing Bromophenol blue (0.05% w/v), EDTA (0.1 M, pH 8.0), sucrose (40% w/v), and SDS (0.5% w/v), and electrophoresed at 90 V for one hour to achieve sufficient resolution. DNA ladders between 100 bp –10 kb range were used to determine the size of visible fragments. Finally, gels were visualized on a ChemiDoc system (BioRad), using Ethidium Bromide (0.5 μg/ml).

2.3 Ligation.

The insert and vector were digested with 1 μl of *EcoRI* (10U) and *NotI* (40U) for 2 hours at 37°C. One μl CIP (10U) was added into the insert reaction for the last 30 minutes. Prior to

the ligation reaction, the digested vector was confirmed by agarose gel electrophoresis and then extracted from the gel using the QIAquick Gel Extraction Kit (Qiagen, Valencia, CA). The insert was purified using the QIAquick PCR purification Kit (Qiagen, Valencia, CA). The ligation reaction was performed at 16 °C for 72 hours. Then, the ligation products were transformed into DH5α competent *E.coli* cells. Positive colonies were selected using ampicillin antibiotic (50 μg/ml) on LB agar plates and plasmids were extracted using the QIAfilter Plasmid Maxi Kit (Qiagen, Valencia, CA).

2.4 Transformation.

Two hundred nanograms of plasmid were added into an aliquot of DH5α (BL21 for protein expression) competent cells. After 20 minutes incubation on ice, heat shock was given at 42°C for 45 seconds (2 minutes for BL21 cells) in a pre-warmed water bath. Cells were incubated on ice for another 2 minutes. Five hundred μl of pre-warmed SOC medium was added to the cells using a proper aseptic technique. Cells were then incubated at 37°C with shaking for 1 hour at 225 rpm. The transformed cells were plated on Luria-Bertani broth (LB) agar plates with ampicillin selection (50 μg/ml) and incubated overnight at 37°C for colony formation. Positive single colonies were used for inoculation of liquid cultures.

2.5 Screening of constructs for presence of insert.

The QIAprep 8 plus TurboFilter Kit (Qiagen, Valencia, CA) was used for purification of up to 20μg plasmid DNA. At least 16 of the positive clones were used for further confirmation of the construct. Each colony was inoculated overnight in 5ml LB with ampicillin (50 μg/ml). Cells were harvested by centrifuging at 4000 rpm for 20 minutes in a Marathon 3200R centrifuge (Fisher Scientific) and pellets were disrupted in resuspension

buffer (50mM Tris-Cl, pH8.0 10mM EDTA; 100 μg/ml RNase A). Cells were lysed using lysis buffer (1% SDS (w/v); 200mM NaOH) and neutralization buffer (3.0M potassium acetate, pH5.5) and plasmids were separated from cell debris by filtration. Plasmids were then eluted and dissolved in 50 μl sterile dH_2O. All 16 samples were digested using EcoRI and NotI for 2 hours at 37°C. Digestion was confirmed by agarose gel electrophoresis. Positive colonies were determined to have correct inserts of the correct size by comparison with a DNA ladder.

2.6 Maxi scale preparation of plasmid DNA.

The QIAfilter Plasmid Maxi Kit (Qiagen, Valencia, CA) was used for purification of up to 500μg ultra-pure plasmid DNA. Two hundred ml LB culture with ampicillin (50 μg/ml) was used for positive construct production. After overnight inoculation, cells were harvested by centrifuging at 6000 rpm for 20 minutes in an Avanti J-25 centrifuge (Beckman). Cell pellets were disrupted in resuspension buffer and plasmids were extracted using lysis and neutralization buffer. After filtering out cell debris, plasmids were washed twice using 30 ml wash buffer (1.0 M NaCl; 15% isopropanol (v/v); 50mM MOPS, pH7.0) and then precipitated using iso-propanol. Finally, the purified plasmids were dissolved in 200 μl sterile dH_2O and concentration was examined by the $OD_{260/280}$ test.

2.7 Site-Directed Mutagenesis.

2.7.1 Mutant strand synthesis PCR.

Two complimentary oligonucleotides (CGGTTGTGAAGAGAAAGCCAAAAA GAATGCCAACAAGCCTTTGCTGGATGAGATTGTGCC and GGCACAATCTCATCCA GCAAAGGCTTGTTGGCATTCTTTTTGGCTTTCTCTTCACAACCG) containing the

desired mutation flanked by unmodified sequence were obtained by purchase (Invitrogen, Carlsbad, CA) and used as primers in PCR. The mutant construct produced as described above was used as the dsDNA template. PCR was performed for 18 cycles of denaturation (95°C, 50 seconds), annealing (60°C, 50 seconds), and extension (68°C, 1 minutes) using *PfuTurbo* DNA Polymerase (Invitrogen, Carlsbad, CA).

2.7.2 *DpnI* digestion of parental (nonmutated) supercoiled dsDNA.

One μl (10U) of *Dpn* I restriction enzyme was added into the amplification product that includes both parental and newly synthesized construct. The mixture was centrifuged for one minute at 1000 rpm, and then immediately incubated at 37°C for 1 hour to digest parental dsDNA.

2.7.3 Transformation of DH5α competent cells.

The transformation reaction was performed as indicated in section 2.3, except that 2 μl of beta-mercaptoethanol (beta-ME) was added into the competent cells prior to the addition of DNA.

2.8 Sequencing.

All cDNA constructs were validated by full-length sequencing. The sequencing primers were designed based on cDNA of human ACBD3 according to the NCBI database. The sequencing process was performed by the Greenwood Molecular Biology Facility, at the University of Hawaii. The cDNA sequence was translated to amino acid sequence and checked for correspondence to the published protein. Protein structure and function was predicted by Swiss Prosite database.

	ACBD3 sequencing primers
F1	TTGTCCTGAGGTTGGATTC
F13	GGAGGAAGAGGAAAGGAGAC
F27	GCAGGAGCAACACTATCAGC
F38	AAGAAGCCCTGGAGAATGGACC
F43	TGACATTGGGTTTGGGGTG
F59	ATGAGGAGGTGTATGCTGGC
R71	CATTCTCTCCTCCTGTCATTC
R72	GAAAAGAGATGGCAACACC

Table 2.8.1. Sequencing primers for ACBD3 cDNA. "F" for forward and "R" for reverse.

2.9. Expression and induction of His-tagged ACBD3 fusion protein.

The *E.coli* BL21 strain was used for expression of fusion protein. Cells were cultured at 37°C in 10ml LB with ampicillin (50 μg/ml) overnight. Cultures were then transferred into 2 X 400ml LB with ampicillin (50 μg/ml) in a ratio of 1:80 followed by 4 hours growth till OD_{600} reaches 0.6-0.8. After removal of 1ml uninduced culture as control, IPTG was added to a final concentration of 0.4 mM to induce expression. After an additional 2 hours growth, cells were harvested by centrifuge at 6000 rpm for 20 minutes in an Avanti J-25 centrifuge (Beckman). The pellets were stored at -20°C overnight.

2.10. Purification of His-ACBD3 by affinity chromatography.

2.10.1 Lysate preparation.

The pellet was thawed at room temperature and disrupted mechanically without adding buffer. After the addition of 40ml binding buffer, the pellet was resuspended completely by pipetting up and down. The proteinase inhibitor cocktail and DNAseI were added to prevent

protein degradation and to reduce viscosity caused by genomic DNA, respectively. The homogenous lysate was sonicated using VCX600 sonicator (Sonics & Materials Inc.) at 50% power for 30 seconds at 4°C. The sonication was repeated eight times, with 1 minute on ice intervals. The lysate was frozen at -80°C overnight.

2.10.2 Purification of the His-tagged ACBD3 fusion protein.

The lysate was thawed at room temperature and centrifuged at 14,000 *g* in an Avanti J-25 centrifuge (Beckman) centrifuge for 20 minutes. The supernatant was filtered through a 0.2 μm filter in order to further reduce viscosity. Five ml of sterile water was first applied to the column to moisten the beads that are attached to the column. An additional 2ml of 50% slurry beads were added. The beads were purchased from Novagen, CA. After all beads settled down, 3ml sterile water, 5 ml charge buffer and 3ml binding buffer were poured throughout the column to charge Ni^{2+} on the beads. The column was loaded with supernatant, and then washed with 10ml binding buffer and 6ml wash buffer. Finally, 6 ml elution buffer was applied to the column and collected as six 1ml aliquots. All buffers and supernatant passed through the column by gravity flow.

2.10.3 Dialysis to remove imidazole contaminant in the eluted sample.

The eluted supernatant was carefully transferred into 3500 MWCO (molecular weight cut off) dialysis tubing and dialysed against 2L PBS for 72 hours at 4 °C. The dialysis tubing had been prepared by boiling in 70% EtOH, and was soaked in dH_2O for at least 1hour prior to use. Dialysis buffer was changed every 12 hours. The dialysed protein sample was transferred into a 15ml falcon tube and stored at 4°C.

2.11 Recoupling the His-tagged ACBD3 fusion protein to the agarose

beads.

One and a half ml of 50% slurry beads were pre-charged using charge buffer and added to dialysed protein sample for 30 minutes incubation at 4 °C. After 3 washes with 6 ml PBS and a wash with 2 ml storage buffer, the supernatant was carefully removed. The beads were transferred into two 2ml centrifuge tubes, followed by two additional washes with 1ml storage buffer. For long term storage, beads were stored in 1 ml storage buffer at -20°C.

2.12 Sodium dodecyl sulphate-polyacrylamide gel electrophoresis (SDS-PAGE).

The acrylamide resolving gels used were 10% with 1% (v/v) SDS, unless otherwise indicated in the figure legends. Electrophoresis was performed at 50-60 volts for 12-16 hours.

2.13 Coomassie Blue Staining.

Gels were immediately soaked incoomassie staining buffer for 2-4 hours after removing from the gel apparatus, and were then destained in destaining buffer until clear bands could be seen. Composition of staining and destaining buffer are as follows: Staining buffer was 0.1% (w/v) coomassie brilliant blue R-250, 10% (v/v) glacial acetic acid, and 10% (v/v) methanol. Destaining buffer was 10% (v/v) glacial acetic acid and 10% (v/v) methanol.

2.14 Electro-transfer and Western blot.

Resolved proteins were transferred fromcrylamide gels to PVDF membranes by electroblotting in the transfer buffer at 1.4 A for 200 minutes at 4 °C. Then, membranes were blocked by non-fat milk solution (5% w/v in PBS) at room temperature for 1 hour with

gentle shaking. Primary antibodies were dissolved in PBS with 0.05% (w/v) Tween-20, 0.02% (w/v) sodium azide, and 0.5% (w/v) BSA, and incubated with the membrane at 4°C overnight. Secondary anti-mouse IgG antibodies were dissolved in PBS/0.05%tween-20/0.5% non-fat milk and incubated with membrane at room temperature for 1 hour. Washes between incubations were performed in 50ml PBS/0.05% Tween-20 for 5 minutes and repeated four times. Finally, membranes were exposed to ECL plus solution for 4 minutes and wrapped in Saran wrap. Signals were visualized using Kodak Biomax MR film. The Western blot array used in Chapter 5 was from Biochain, Inc.

2.15. Antibodies.

Antibodies to His-tag were from Invitrogen, Carlsbad, CA.

ACBD3 antibody was from Dr. Papadopoulos, Georgetown University, Washington DC.

2.16. *In vitro* PKA binding assay.

Purified human recombinant Protein Kinase A, and Protein Kinase G were obtained from Promega. Recombinant kinases were stored as aliquots at -80 degrees C, in a buffer containing 20% (w/v) glycerol at pH 7. Affinity purifications of ACDB3 with recombinant PKA or PKG were performed as follows by Dr. Turner and this candidate. His-ACBD3 was coupled to $NiCl_2$ affinity matrix (Novagen, CA) as described above. After washing, and estimation of coupled protein concentration by SDS-PAGE, the affinity matrix was resuspended in a buffer containing 10mM Tris-HCl pH 7.4, 75mM NaCl, 1mM phenylmethylsulfonyl fluoride and 10mM iodoacetamide. Eppendorf tubes were prepared containing 10μg of the coupled His-ACBD3. Candidate interacting proteins were included in the reaction mixture at the concentrations indicated in the figure legends. Affinity

purification proceeded for 2h at 4 °C on a rotator, in a reaction volume of 500 µl. After affinity purification, the protein complexes were harvested by centrifugation (15,000 *g* for 1 min at RT), followed by three washes in 1 ml volumes of ice-cold PBS. After the final wash, the beads were dried using a Hamilton syringe and resuspended in 100 µl of reducing Laemmli sample buffer. Samples were heated at 95 °C for 8 min, before loading on a 10% SDS-PAGE gel. Protein complexes were electrophoresed for 16 h at 60 V, before fixation and staining of the gel with Coomassie Blue.

Table 2.1.1 List of Buffers used in protein analysis

Buffer	Component
Binding buffer	0.5M NaCl; 20mM Tris-HCl; 5mM imidazole;pH7.9
Charge buffer	50mM NiSO4
Elute buffer	1M imidazole; 0.5M NaCl; 20mM Tris-HCl; pH7.9
Laemmli sample buffer	60mM Tris(pH6.8); 1.5%SDS; 10% glycerol; 0.01% Bromophenol Blue; 5% 2-mercaptoethanol (b-ME)
PBS buffer	phosphate-buffered saline
Running buffer	25 mM Tris, 0.2 mM Glycine, 0.1 % SDS, pH 8.3
Storage buffer	50% w/v glycerol; 50mM NaCl; 50mM Hepes;pH7.4
Transfer buffer	25 mM Tris, 0.2 mM Glycine, pH 8.3
Wash buffer	0.5mMNaCl; 60mM imidazole; 20mM Tris-HCl; pH7.9

Table 2.1.2 Reagents or kits and their suppliers

Reagent or kit	Supplier
AccuPrime™ *Pfx* SuperMix	Invitrogen
Autoradiography Film	Kodak
Calf intestinal phosphatase (CIP)	Invitrogen
DNaseI	Sigma
ECL plus	Amersham
oligonucleotide primers	Invitrogen
PfuTurbo DNA Polymerase	Invitrogen
protease inhibitor	Calbiochem
purification kit	Novagen
PVDF	Millipore
QIAfilter Plasmid Maxi Kit	Qiagen
QIAprep 8 plus TurboFilter Kit	Qiagen
QIAquick Gel Extraction Kit	Qiagen
QIAquick Gel Extraction Kit	Qiagen
QIAquick PCR purification Kit	Qiagen
Restriction Enzymes	New England Biolab
SDS solution	BioRad

Chapter 3

Subcloning, expression and induction of ACBD3

3.1 Goal.

As described in the introduction, our ultimate goal is to identify the cellular targets for the AKAP anchoring of ACBD3 protein. Our chosen approach is to generate purified ACBD3 protein that will be used as an affinity matrix to co-purify interacting partners for ACBD3 protein.

The first step of this process is to identify a system for production of the His-tagged ACBD3 fusion protein. Bacterial expression systems yield high concentrations of soluble proteins like ACBD3. To facilitate purification and detection of ACBD3, we decided to engineer a minimal peptide tag (6 sequential Histidine residues) onto the ACBD3 protein. This chapter will describe the production by PCR of the His-ACBD3 open reading frame, and its subcloning into a cDNA vector that is suitable for production of recombinant protein in *E.coli*.

The *E.coli* expression system is one of the best understood systems for heterologous protein expression. The advantages of the *E.coli* expression system include established regulatory track record, well-understood genetics, ease of culture, inexpensive media, high and regulated expression levels, and relatively easy characterization. It offers a reliable and cost effective way of expressing genes of interest. Many *E.coli* strains have been engineered

to be particularly useful for high level protein expression. The BL21 strain is one of the general protein expression strains that lack both the *lon* protease and the *ompT* membrane protease, which can degrade proteins.

The pTrcHisB expression vector is useful because it confers a His-tag sequences and allows inducible production of His-tagged protein. To achieve stringent control of expression, the *lac* operator has been engineered into the pTrcHisB vector, which permits binding of the Lac repressor to repress transcription. When expression is desired, the *E.coli* are grown to mid-log phase (OD_{600}=0.6-0.8) and IPTG is added to induce expression via de-repression. Translation is enhanced by the presence of a minicistron that provides highly efficient translational restart into the open reading frame of the multiple-cloning site. ACBD3 insert is positioned downstream of the minicistron and in frame with a sequence that encodes an N-terminal fusion peptide. This N-terminus peptide codes for (5' to 3' from the promoter) an ATG translation initiation codon, six histidine residues in series that function as a metal (Ni^{2+}) binding domain in the translated protein, the Xpress epitope, and the enterokinase cleavage recognition site. The enterokinase cleavage recognition site allows for the subsequent removal of N-terminal fusion peptide from purified recombinant protein.

3.2 Results.

3.2.1 Subcloning of ACBD3 cDNA into pTrcHis B vector.

The human ACBD3 cDNA (accession ID: BC060792) has 1588 base pairs. We chose to subclone ACBD3 into the pTrcHisB vector. The pTrcHisB vector (Figure 3.2.1) is a pBR322 derived expression vector and is designed for efficient His-tagged protein expression and purification in *E.coli*. The overall subcloning strategy is presented in Figure 3.2.2. The

subcloning results including PCR, vector digestion and mini-prep confirmation are shown in Figure 3.2.3-5. The samples in lane 9 and 11 in figure 3.2.5 were used for bulk cDNA preparation and confirmation of the subcloning by DNA sequencing.

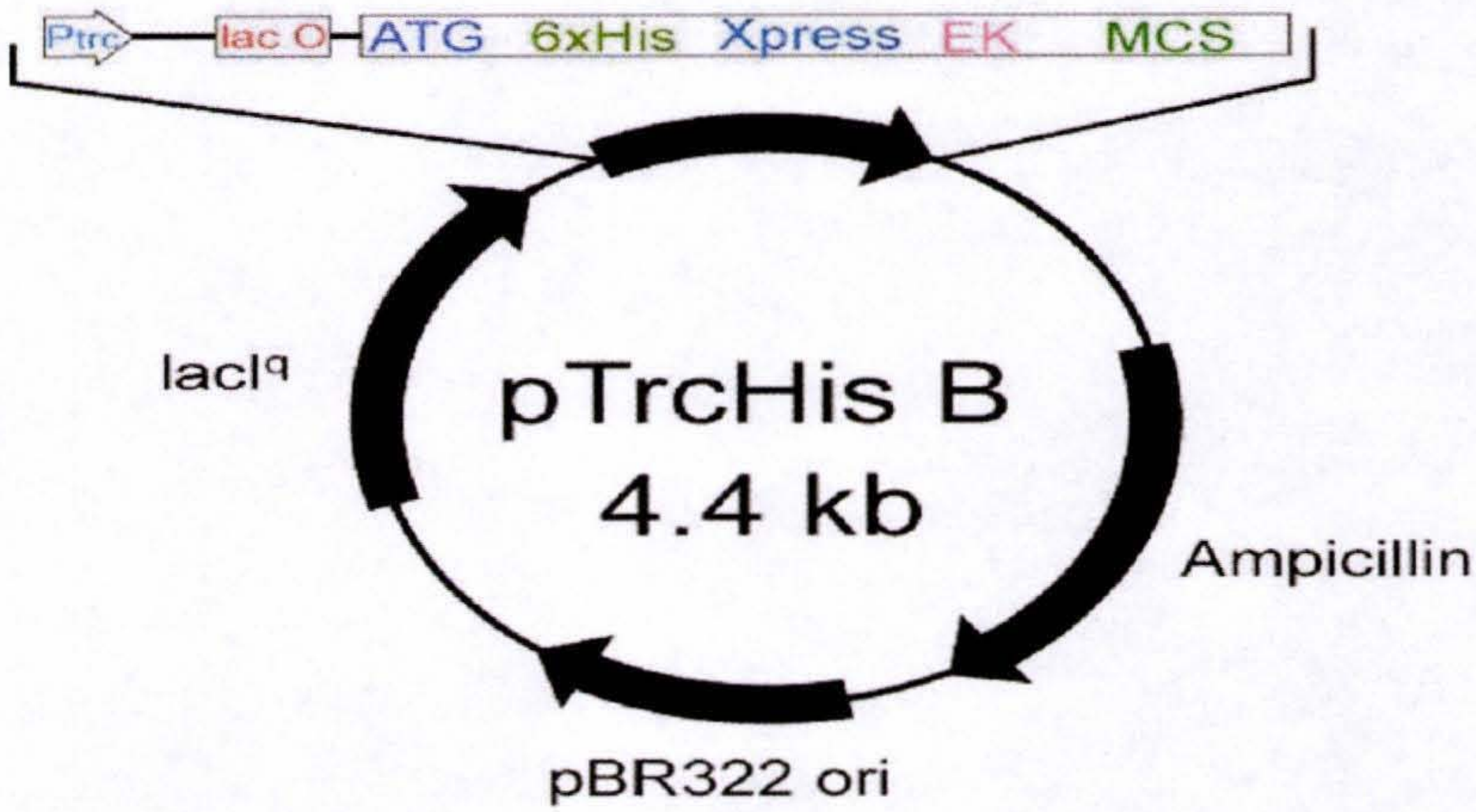

Figure 3.2.1 pTrCHisB vector map. pTrcHisB vector is a 4.4kb vector that contains pBR322 origin of replication. Six histidine residues, the Xpress epitope, and the enterokinase cleavage recognition site are in frame between the A TG translational start codon and multiple cloning site.

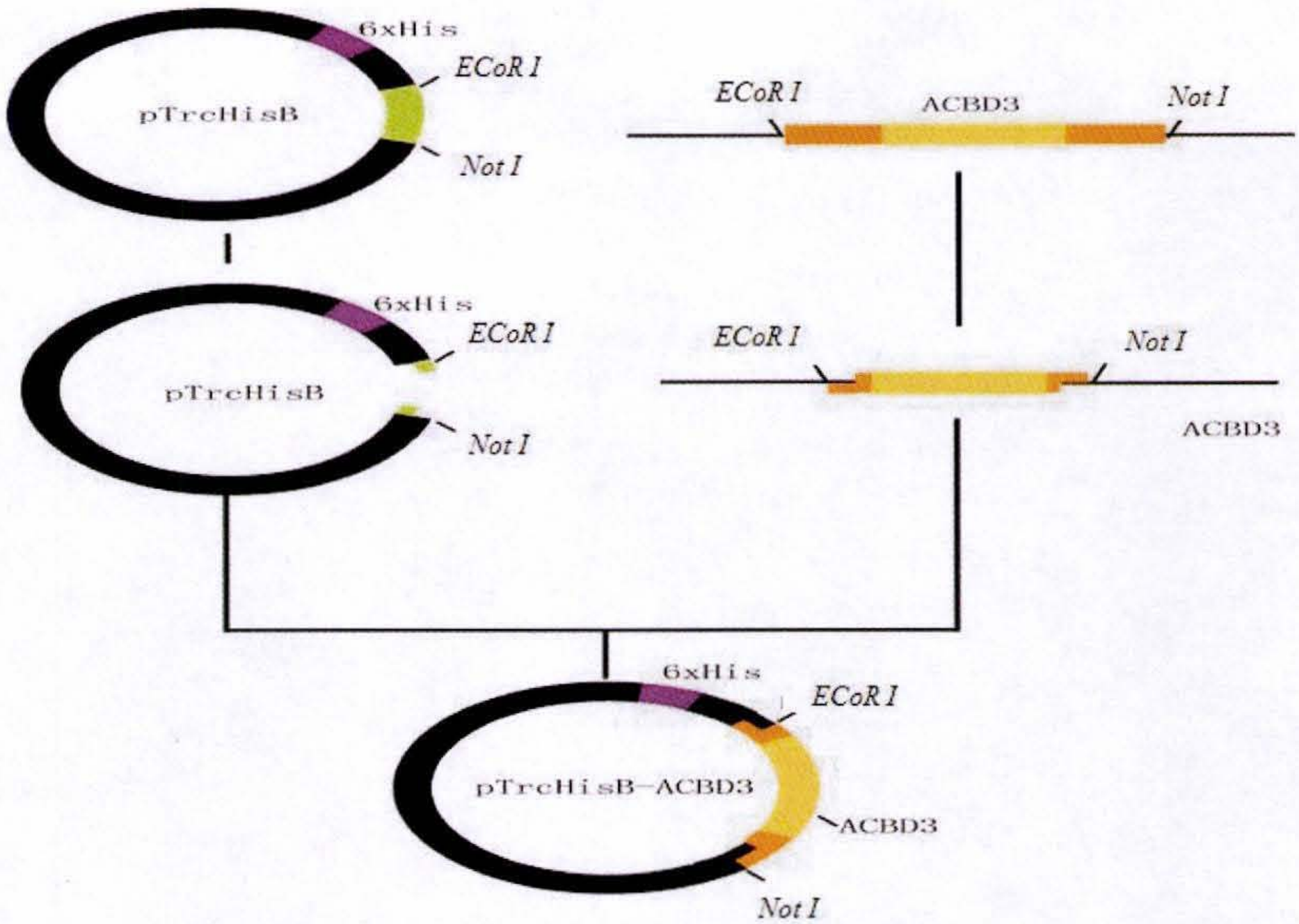

Figure 3.2.2 Subcloning strategy for ACBD3. The insert is produced by PCR and purified from an agarose gel. The vector is purified using maxi prep. Both insert and vector are treated with *ECoR I* and *Not I* for two hours prior to ligation reaction. Yellow: ACBD3 cDNA; Orange: restriction enzyme site; Green: multiple cloning site; Purple; six histidine residues.

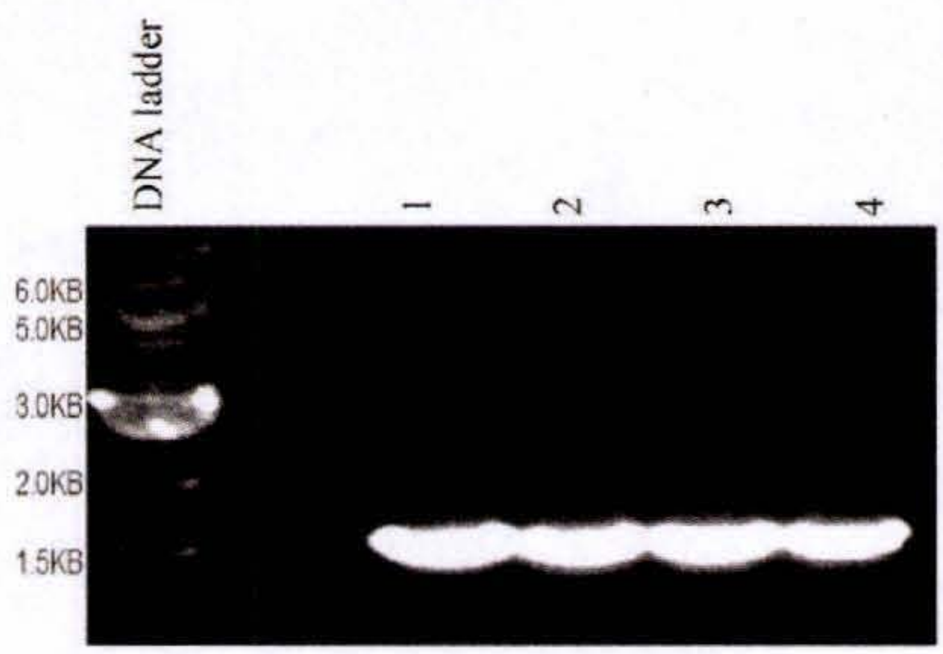

Figure 3.2.3 PCR product of ACBD3. Agarose gel (1%) electrophoresis of PCR product of ACBD3 cDNA. Lane 1-4 represent four trials in the same thermocycle. PCR product of ACDB3 is 1588 bp and observed at 1.5 kb. Sizes of fragments were estimated by comparison to DNA ladder shown on left. The gel was visualized on a ChemiDoc system (BioRad) using Ethidium Bromide (0.5 μg/ml).

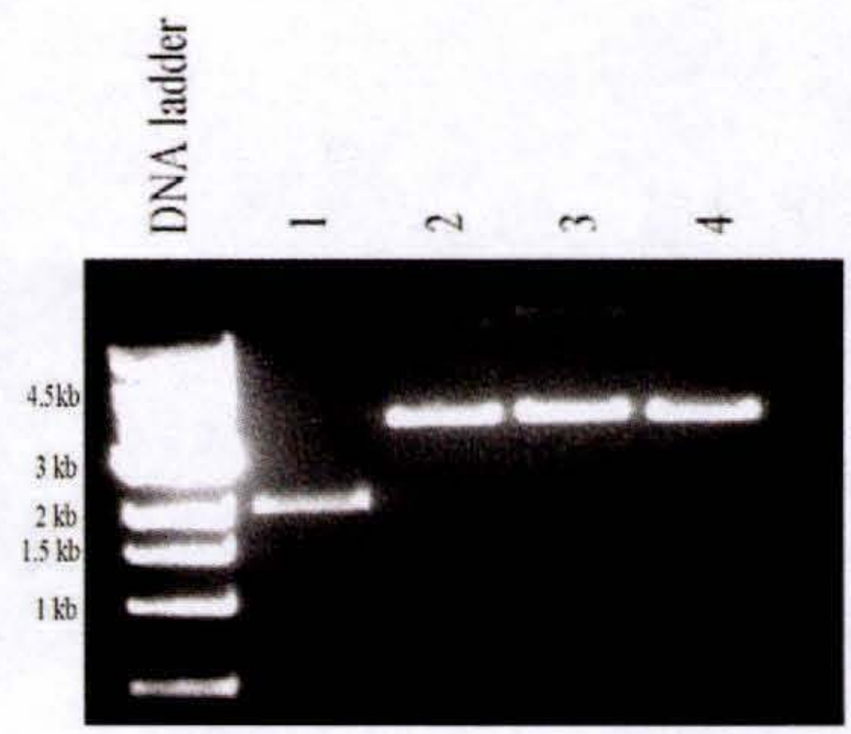

Figure 3.2.4 Restriction enzyme digestion of pTrcHisB vector. Agarose gel (1%) electrophoresis of digestion of pTrcHisB vector by restriction enzyme. Lane 1: vector alone; Lane 2: vector and EcoR I; Lane 3: vector and Not I; Lane 4: vector, EcoR I and Not I. The digestion was performed as indicated at 37° C for 2 hours. Sizes of fragments were estimated by comparison to DNA ladder shown on left. The gel was visualized on a ChemiDoc system (BioRad) using Ethidium Bromide (0.5 μg/ml).

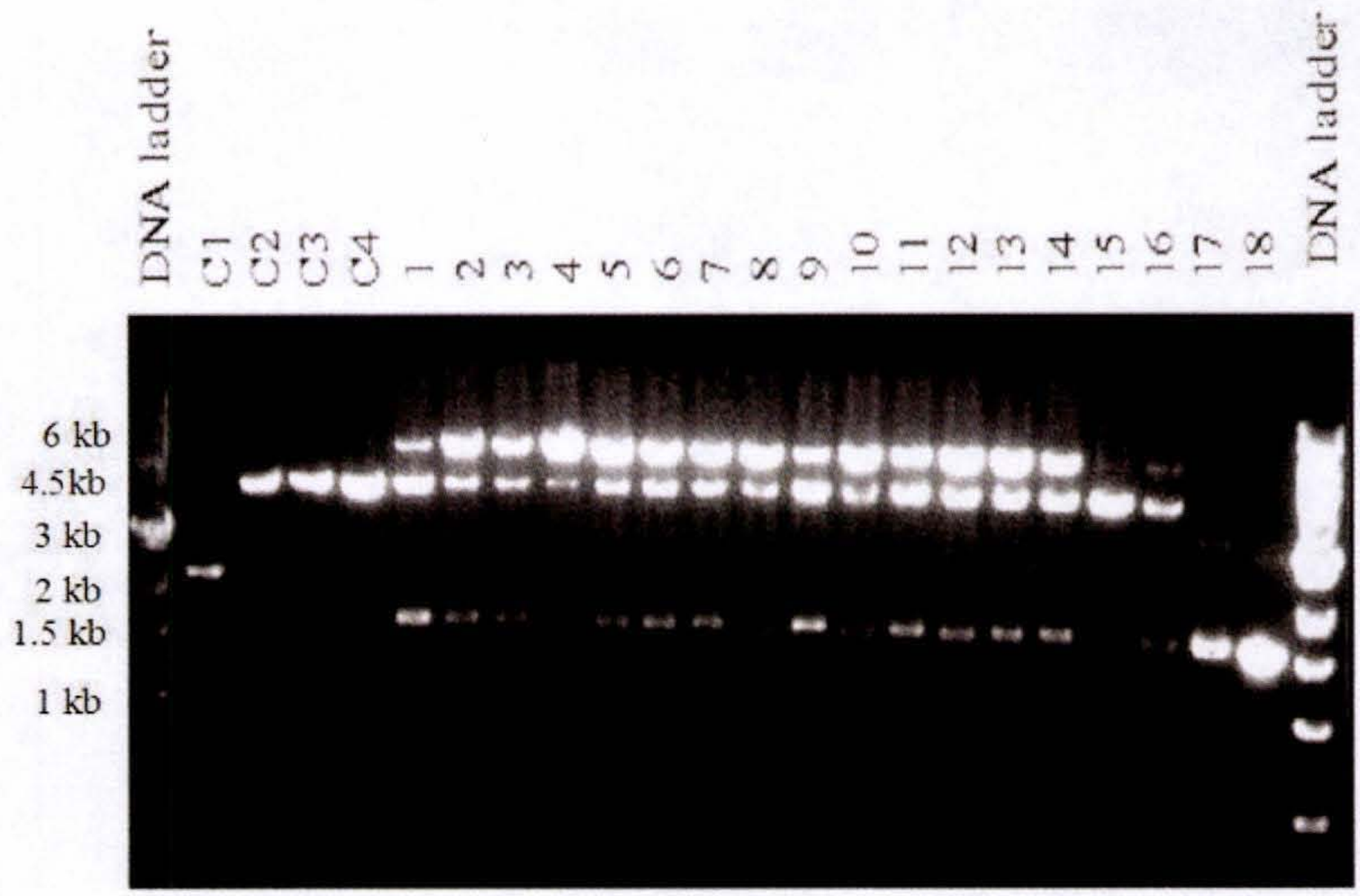

Figure 3.2.5 Restriction enzyme digestion of ACBD3-pTrcHisB constructs. Agarose gel (1%) electrophoresis of digestion of ACBD3-pTrcHisB constructs by restriction enzymes. C1-C4 are control. C1: vector alone; C2: vector and EcoR I; C3: vector and Not I; C4: vector, EcoR I and Not I. Lane1-18: 18 mini-prep samples The digestion was performed as indicated at 37° C for 2 hours. Sizes of fragments were estimated by comparison to DNA ladder shown on left and right. After digestion, the inserts are observed as about 1.5 kb and the vectors are observed as about 4.5 kb fragment. The gel was visualized on a ChemiDoc system (BioRad) using Ethidium Bromide (0.5 mg/ml).

3.2.2 Site-directed mutagenesis of ACBD3-pTrcHisB construct

According to the NCBI database, the ACBD3 cDNA used in this experiment has one base pair that is different from human genome, which results in a change of the 473rd amino acid from arginine to lysine. The shift of even one amino acid may cause the protein function irregularly due to many possible reasons, such as a change in structure or in a site for post-translational modification. Therefore, in order to repair this mutation, a single base

pair change was been made in the ACBD3-pTrcHisB construct.

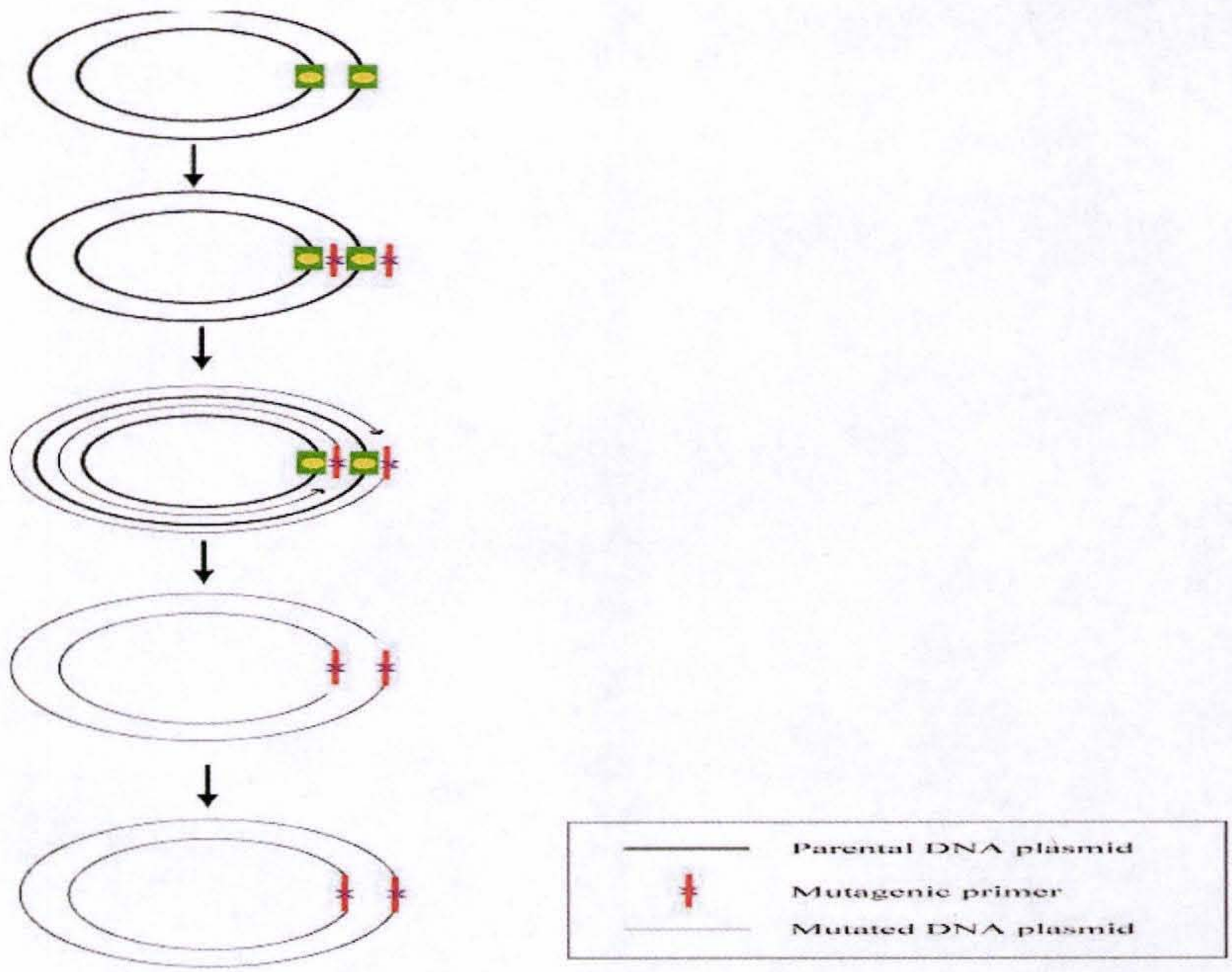

Figure 3.2.6 Schematic of site directed mutagenesis. Parental plasmids are mutated by PCR amplification using mutated primers. The two primers are reverse and complementary to each other. After PCR, the parental plasmids are digested using *Dpn I* restriction enzyme.The mutated plasmids survive from digestion and are selected for use.

The site-directed mutagenesis allows site specific mutations in virtually any double stranded plasmid. As described in the Methods, site-directed mutagenesis is performed using *PfuTurbo* DNA polymerase and a temperature cycle. The *PfuTurbo* DNA polymerase replicates both plasmid strands without displacing the mutant oligonucleotide primers. The

basic procedure utilizes a supercoiled double stranded DNA vector with an insert of interest and two synthetic oligonucleotide primers containing the desired mutation. The two oligonucleotide primers, each complementary to opposite strands of the vector, are extended through a temperature cycle by *PfuTurbo* DNA polymerase. A mutated plasmid containing staggered nicks is generated by incorporation of such primers. The product is treated with *DpnI* endonuclease, which is specific for methylated and hemimethylated DNA. Since DNA isolated from almost all *E.coli* strains is methylated, *DpnI* treatment is used to digest parental DNA template in order to select for the mutation-containing synthesized plasmid. The new construct, with the single base pair change, is confirmed by sequencing.

bp	1383	1384	1387	1390	1393	1396	1399	1402	1405	1408	1411	1414	1417	1420	1423	1426	1429	1432	1435	1438	1440
	*	*	*	*	*	*	*	*	*	*	*	*	*	*	*	*	*	*	*	*	*
	C	GGT	TGT	GAA	GAG	AAA	GCC	AAA	AAG	AAT	GCC	AAC	AAG	CCT	TTG	CTG	GAT	GAG	ATT	GTG	CC
	C	CCA	ACA	CTT	CTC	TTT	CGG	TTT	TTC	TTA	CGG	TTG	TTC	GGA	AAC	GAC	CTA	CTC	TAA	CAC	GG
wt-aa	*	G	C	E	E	K	A	K	K	N	A	N	K	P	L	L	D	E	I	V	*
mutation													R	to be mutated							
mutation primer1	C	GGT	TGT	GAA	GAG	AAA	GCC	AAA	AAG	AAT	GCC	AAC	AGG	CCT	TTG	CTG	GAT	GAG	ATT	GTG	CC
mutation primer2	C	CCA	ACA	CTT	CTC	TTT	CGG	TTT	TTC	TTA	CGG	TTG	TCC	GGA	AAC	GAC	CTA	CTC	TAA	CAC	GG

Table 3.2.2 ACBD3 site-directed mutagenesis. An "A-T", the 1418th base pair of ACBD3 cDNA, is mutated to a "G-C". Consequently, the amino acid is shifted from lysine to arginine, corresponding to the human genome reference sequence for ACBD3.

3.2.3 Expression and induction of His-tagged ACBD3 fusion protein.

After transformation of the repaired construct containing the pTrcHisB plasmid, the BL21 expression system provided sufficient but not excessive amounts of Hig-tagged ACBD3 fusion protein when induced with IPTG. With the combination of pTrcHisB plasmid and BL21 strain, His-tagged ACBD3 expression in conditions of presence and absence of IPTG induction was confirmed using Coomassie Blue staining. Figure 3.2.7 shows the expression and induction of this protein.

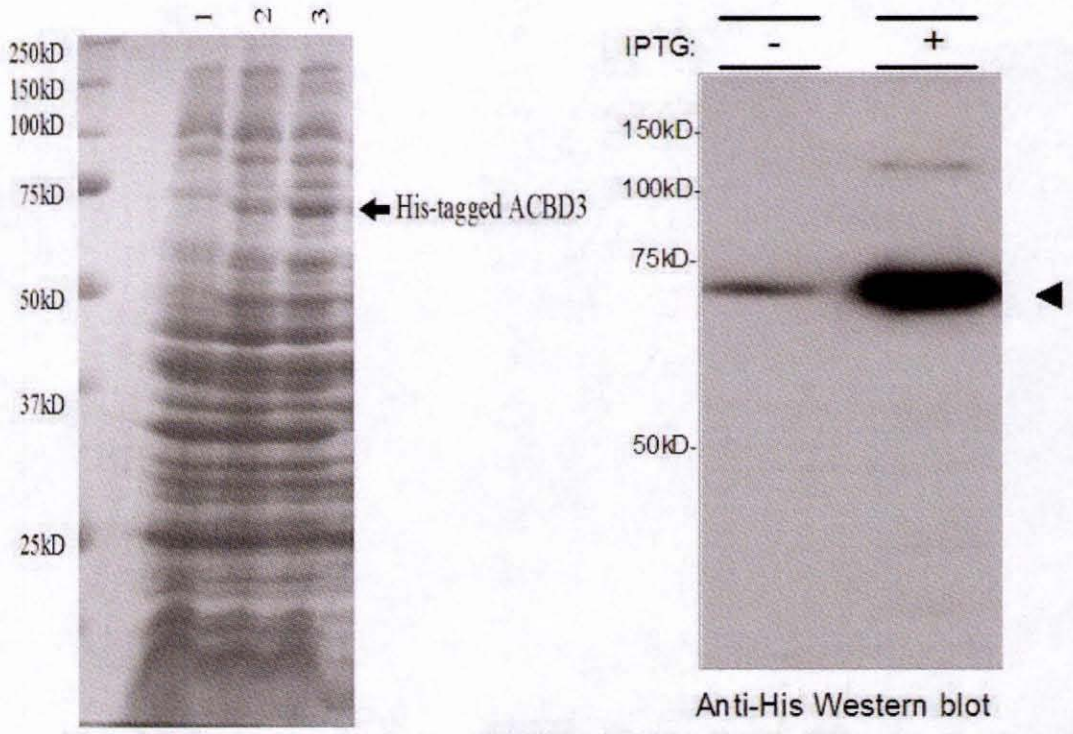

Figure 3.2.7 Expression and induction of ACBD3 in BL21 *E.coli* strain. Total proteins from bacterial cells were loaded on 10% SDS-PAGE. The gel is visualized by Coomassie Blue staining for 4 hours and followed by destaining. One ml of culture wsa used for confirmation of pretein expression and induction. Lane1: total proteins from BL21 strain without transformation of ACBD3-pTrcHisB construct. Lane2: total proteins from Bl21 strain with transformation of ACBD3-pTrcHisB construct. Lane3: total proteins from BL21 strain with transformation of ACBD3-pTrcHisB and induced by IPTG. His-tagged ACBD3 fusion protein is observed as about 70 kD fragment and indicated by arrow.

3.3 Discussion.

Our subcloning strategy resulted in a successful production of a construct. The whole subcloning process was straightforward until we found there was a point mutation of the cDNA that has been used in the PCR. This mutation is due to the original source of Open Biosystem's construct, which is contained this difference between human ACBD3 cDNA and genomic DNA. We dealt with this problem using a site directed mutagenesis technique and made our construct correspond to the predicted protein from the human genome.

In the follow-up step, expression and induction were quite straightforward comparing with previous work on other projects. The solubility and degradation problem of expressed fusion protein were easily resolved using our experiences gained from other projects. For example, we monitored the protein expression and induction by SDS-PAGE and Coomassie Blue staining. In the first several trials, we found that the majority of expressed His-tagged ACBD3 was in lysed samples but not in the supernantants of them. This phenomenon is due to two potential problems: (1) The heterogeneously expressed proteins were poorly soluble; (2) The lysis and exaction of protein from bacterial cells were not sufficient. However, this problem was easily dealt by inducing at an early time and shortening the induction period, which proved that the problem was due to the problems mentioned above.

Chapter 4

Purification of His-tagged ACBD3

4.1 Goal.

The goal of the work presented in this Chapter is to purify His-tagged ACBD3 fusion protein from BL21 *E.coli* cells. Our overall goal of this study is to use purified His-tagged ACBD3 to identify its interactors by affinity purification. Therefore, generating a tool of purified His-tagged ACBD3 fusion protein is the key step of the entire project. Our chosen strategy is to use the Immunobilized Metal Affinity Chromatography (IMAC) technique. IMAC is a widely used method for purifying large quantities of highly pure protein in a single process. This technique also allows purification under both native and denaturing conditions.

The work presented in this chapter also includes the preparation for further affinity purification experiment. The affinity purification requires the purified His-tagged ACBD3 fusion protein to be coupled onto a bead matrix. Therefore, we dialyzed the eluted sample and recoupled the protein to beads.

4.2 Results.

4.2.1 Purification of His-tagged ACBD3 by Immunobilized Metal Affinity Chromatography

The entire purification system is facilitated by two different binding affinities between histidine residues to Ni^{2+} beads and imidazole. Beads were first charged by Ni^{2+} before binding to the His fusion protein. When the His-ACBD3 protein is pulled down through the Ni^{2+} beads, strong binding affinity between histidine residues and Ni^{2+} allows His-ACBD3 tethering to the beads. After several washes, the elution solution containing imidazole is pulled down through the Ni^{2+} beads with the bound His-ACBD3 fusion protein. As imidazole has a higher affinity to histidine residues than Ni^{2+} beads do, the His-ACBD3 is eluted in the elution buffer.

Total soluble protein was first extracted from BL21 cells and then the His-tagged protein was purified by immobilized metal affinity chromatography (Figure 4.2.1).

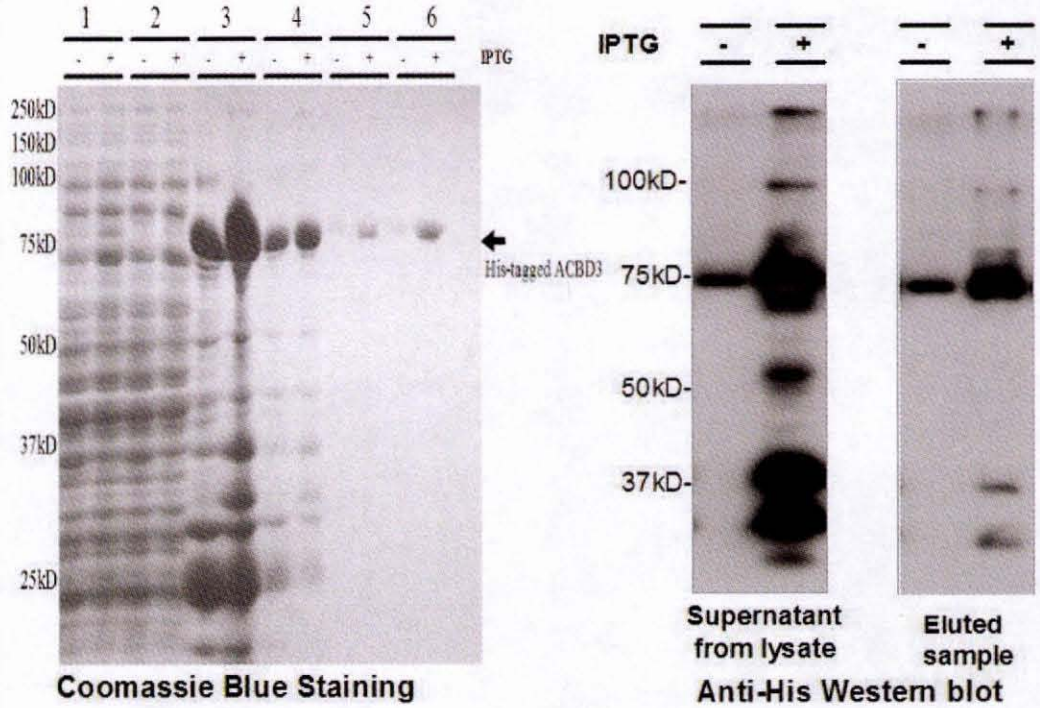

Figure 4.2.1 Purification of His-tagged ACBD3 fusion protein. Total proteins from bacterial cells were loaded on 10% SDS-PAGE. The gel is visualized by Coomassie Blue staining for 4 hours and followed by destaining. 30 μl of total lysate was loaded in lane1. After centrifugation, supernatant was loaded in Lane2. After coupling to His-tagged ACBD3 fusion protein, 10 μl of beads was load in lane 3 before elution. After elution, 50 μl of first and second eluted and 100 μl of third eluted sameles were loaded in lane 4-6, respectively. His-tagged ACBD3 fusion protein was observed as a 70 kD protein and indicted by arrow.

4.2.2 Re-coupling of purified protein to beads.

To eliminate the potential effect of imidazole contaminating the eluted sample, His-tagged ACBD3 fusion protein was re-coupled to the beads after dialysis against PBS. The dialysis system chosen used a cellulose membrane with a molecular weight cut off of 3500 Dalton. Thus, the purified protein, which is about 50kDa, would be retained in the dialysis tube while imidazole, whose molecular weight is about 250 Dalton, would be diluted into the surrounding PBS.

At this point, we had a very diluted sample of the His-tagged fusion protein. The next step is to re-couple to beads, concentrating the protein, which is our affinity ligand, onto a solid matrix where it can be used in affinity purification. The His-tagged ACBD3 fusion

protein was recoupled onto the Ni^{2+} beads by incubation of the beads in the dialyzed protein sample. Efficiency of coupling was assessed by SDS-PAGE of the recoupled beads and the dialysate after this re-coupling. Figure 4.2.2 shows that high efficiency re-coupling was achieved.

Figure 4.2.2 Recoupling of His-tagged ACBD3 to Ni2+ coupled beads. All samples were loaded on 10% SDS-PAGE followed by Coomassie Blue staining. Lane 1: 10 µl of eluted sample after purification; lane2-5: 50 µl of washing buffer after passed through the beads; Lane 6: 20 µl of beads after recoupling; The gel was visualized by Coomassie Blue staining for 4 hours and followed by destaining.

4.3 Discussion.

4.3.1 Degradation of the protein in the *E.coli* expression system.

Being able to synthesize the fusion protein without excess degradation is one of the most important considerations in experiment design. If the fusion protein is excessively

degraded during purification, the probe protein will be a mixture of different products of degradation. This may result in variable results from different fusion protein preparations. The *E.coli* expression system is apt to generate degraded products during over-expression. The BL21 strain used in the experiment was engineered as a protease deficient (lon^-) strain. This strain was selected for protein expression with an appropriate genetic background to minimize protein degradation. We did experience some excessive degradation of protein during the experiment (data not shown). The excessive degradation showed increased amount of degraded products and decreased amount of full length protein. Degradation is supposed to take place due to various stresses to the bacteria including over induction, long period culture and so on. Degradation may also result from over sonication. However, sonication is necessary to disrupt cell walls and to help protein extraction. Therefore the duration and strength of sonication should be balanced between extraction and degradation. Figure 4.2.1 is the most representative data we have to show minimized degradation and optimized purification.

4.3.2 Insolubility of the expressed fusion protein.

The fusion proteins can be produced either as soluble forms and/or as insoluble forms (inclusion body) in *E.coli* expression system. The formation of inclusion body is a common consequence of high level protein expression in cytoplasm. So far, there is no evidence on why fusion proteins tend to form inclusion body in *E.coli*. Moreover, it seems like that no relationship between the formation of inclusion bodies and origin of proteins, choice of promoters, choice of vectors, and the hydrophobicity of target proteins.

To avoid the formation of inclusion body and to increase soluble protein, we tried

several means such as titrating the amount of IPTG added, altering the OD600 when the IPTG is added, lowering the temperature, and inducing for longer or shorter time. However, for His-tagged ACBD3, all above experiments showed no effect on the amount of soluble proteins and inclusion bodies. This proved the choice of His-tagged fusion system was appropriate, instead of GST fusion system, with which we have experienced huge inclusion body and insolubility problems during the protein purification projects.

Chapter 5

Structure-function analysis of The ACBD3 protein

5.1 Goal.

The goal of the work presented in this Chapter is (1) to prove that our His-ACBD3 is a potentially useful affinity ligand. Our approach was to test whether our His-ACBD3 is capable of binding to PKA. If this is successful, then we will have produced a novel affinity ligand for future purification of ACBD3-interacting proteins; (2) to test the idea that ACBD is likely to bind to proteins other than TRRV ion vhannels. These are proteins with restricted tissue expression pattern. So we will ask whether ACBD3 is expressed in non-TRPV containing tissues (outside the CNS). If so, this would support our hypothesis that undescribed partners for ACBD3 are likely to exist.

5.2 Results.

5.2.1 Validation of His-ACBD3 fusion protein via *in vitro* PKA binding assay.

Proteins control and mediate many of the biological activities of cells. Although some proteins may act as single monomeric units, a significant percentage of all proteins function in association with their partners, or as components of large macro-molecular complexes. Therefore, to gain an understanding of cellular function, we think the function of ACBD3 must be understood in context of other interacting proteins.

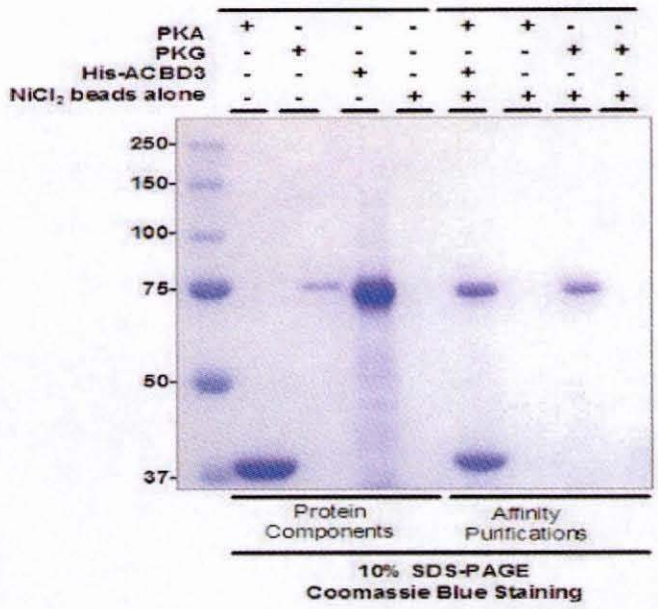

Figure 5.2.1 ***In vitro*** **PKA binding assay of ACBD3.** His-tagged ACBD3 fusion protein was pre-coupled to the beads. Candidate interacting molecules were incubated with beads for 2 hours at 4 ° C. After washes, the beads were boiled at 95 ° C in Laemmli sample buffer and loaded to 10% SDS-PAGE. The gel was visualized by Coomassie Blue staining.

As mentioned in the Introduction, TRPV1 is a heat-transducing and capsaicin sensitive vanilloid receptor. PKA phosphorylation of TRPV1 has been shown to be mediated by AKAP. Results from previous Yeast Two Hybrid experiments have shown that ACBD3 may also mediate the interaction between PKA and TRPV2, another member in TRPV family with a higher threshold than TRPV1. These results suggest that ACBD3 function as an AKAP that mediates the interaction between PKA and TRPVs. To confirm interaction between our His-tagged ACBD3 fusion protein and PKA, an *in vitro* binding assay was performed using purified His-ACBD3 and PKA subunits. As expected, Figure 5.2.1 shows that ACBD3 binds to the PKA R subunit. By binding to PKA, ACBD3 is able to function as a scaffold protein and recruits PKA to its substrates. This result provides the possibility to

extend the AKAP function of His-ACBD3 to other potential interactive partners.

5.2.2. Extensive protein expression pattern of ACBD3.

ACBD3 has only previously been shown to bind TRPV channels (components of CNS and mast cells), and the PBR. In both cases it is likely that ACBD3 is recruiting PKA. However, by analogy to most AKAPs, it is clear that ACBD3 is likely to bind to many other targets and recruit PKA to them. Support for this idea is shown in Figure 5.2.2. Here we performed a Western blot analysis of the distribution of ACBD3 in multiple normal tissues. The anti-ACBD3 antibody was optimised in Western blot by Dr Stokes [30]. Similar blotting conditions were used to probe the total human tissue protein array shown in Figure 5.2.2. It is notable that ACBD3 is abundant in a range of normal tissues, outside the CNS and reproductive organs where the TRPVs and PBR are located. Thus the tissue distribution of ACBD3 in humans is consistent with its function outside the TRPV and PBR pathways. Moreover, it is clear that in certain tissue, ACBD3 levels are altered after oncogenic tranformation. For example, in a clear cell carcinoma of the ovary, ACBD3 levels are massively up-regulated in the transformed tissues.

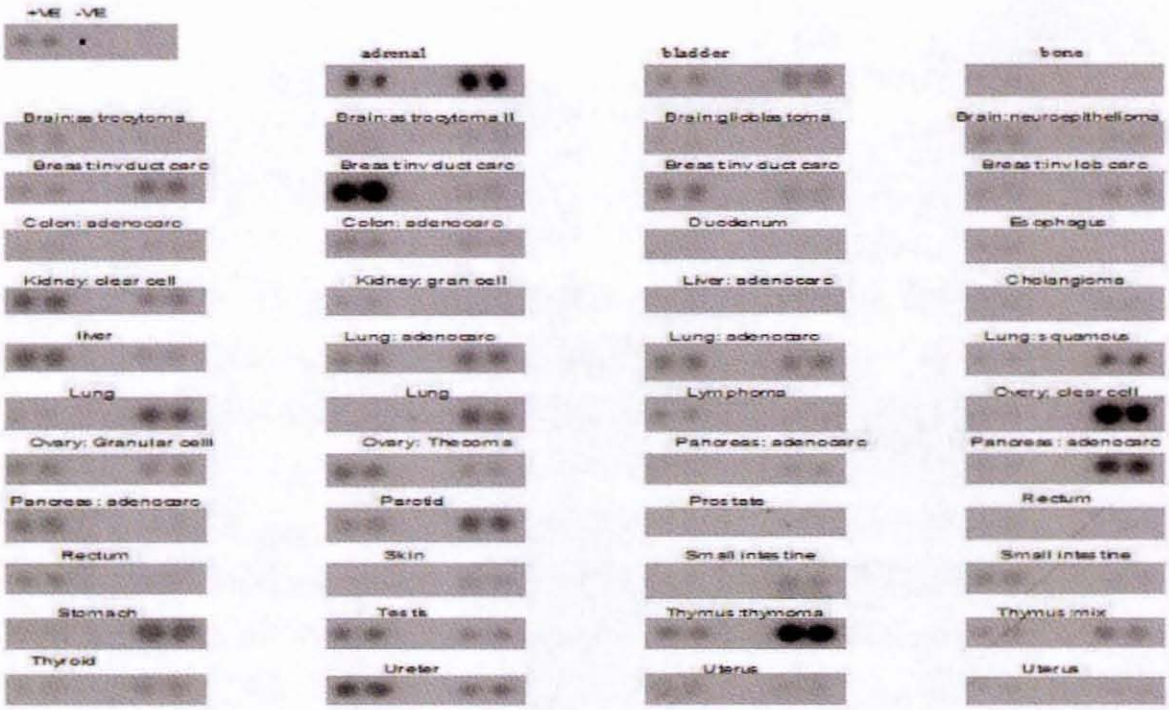

Figure 5.2.2 Expression profile of ACBD3. A Biochain human tissue array blot were probed. Western blot analysis of distribution of ACBD3 in different tissues. All samples were western blotted using anti-ACBD3 antibody. Positive and negative control is in the left top. In each picture, the expression of ACBD3 in oncogenic tissues and normal tissues is shown in the left and right side, respectively.

5.3 Discussion.

By affinity purification using purified His-ACBD3 fusion protein, we were able to confirm the interaction between ACBD3 and PKA R subunit. This interaction seems to be tight and specific. At the beginning, we hypothesized that ACBD3 is a PKA regulator. In addition to the results from previous experiments that were conducted in the laboratory, we know at least ACBD3 is able to regulate PKA to TRPV2 ion channels. Coupling to the knowledge from some members in AKAP family that have been shown as models to regulate PKA to different ion channels, we are able to extend our hypothesis: ACBD3 may recruit PKA to ion channels and proteins other than TRPVs [5, 34-37].

It is important to note that AKAP is defined as a functionally but not structurally related family. The ability to bind to PKA in a specific manner provides ACBD3 the competence to join the AKAP family. According to our bioinformatics prediction of ACBD3 protein, presence of Acyl-CoA binding domain and GOLD domain suggests that ACBD3 are likely to interact with membranes. By occupying the nearby space inside the membrane, ACBD3 is possible to be a scaffold protein that facilitates certain modification of membrane proteins including ion channels. Though the exact localization still needs to be investigated, at least, the prediction based on the domain functions is consistent with our hypothesis.

Our data suggest that ACBD3 expression is not restricted to the CNS and reproductive tissues where it has previously been described. On the Western tissue array used here, it is clear that ACBD3 is present in diverse tissues such as lung, breast and stomach. Moreover, levels of ACBD3 change in cancers of some tissues, although we do not yet know if this is a cause or effect of cellular transformation. Further studies of ACBD3 expression will be needed, since this array technology does not tell us where in the tissue ACBD3 is located. For example, only an immunohistopathology experiment would tell us if the ACBD3 expression is not due to the presence of innervating neurons in the tissues used to prepare this array.

CHAPTER SIX

General Discussion

6.1 Overall summary of the project.

The goal of this project was to generate a tool to purify ACBD3-interacting proteins. No significant technical barriers were encountered. Our study of structure and function relationships as well as protein-protein interactions of ACBD3 started from *in silico* investigation and published results. We successfully produced the His-tagged ACBD3 fusion protein and we purified it by immunized metal affinity chromatography. Using purified His-tagged ACBD3, we could validate the protein-protein interaction between PKA R subunit and ACBD3, suggesting that our His-tagged ACBD3 fusion protein is correctly folded. Protein expression profile of ACBD3 in different tissues was investigated using an anti-ACBD3 antibody. Our results were consistent with our hypothesis, though some further work is still necessary for complete validation. We believe our work has generated a powerful tools for further study of ABCD3 and indicates the right directions for future investigations.

6.2 Future experiments using purified His-ACBD3.

With the purified His-tagged ACBD3, we are now able to probe interactions between ACBD3 and interacting partners in solution. There are two general applications of the affinity purification: 1) to identify novel interactions between ACBD3 and unknown proteins; 2) to confirm interactions between ACBD3 and known proteins that are suspected

interacting partners. For the former, cell lysates from different cell lines can be used to screen potential interacting partners of ACBD3, which can be then identified by mass spectrometry. For the latter, the known interacting partners can be detected by antibodies. We hope, by these affinity purifications, to be able to identify new interacting partners for ACBD3, especially ion channels.

In recent years, electrophysiological tools have been a popularly used in the study of ion channels. Although ACBD3 is responsible to regulation of TRPV phosphorylation, its mechanism is still to be clearly understood. If cell lines that expressing different ion channels are available, we can address the question that if ACBD3 also regulates other ion channels as well as TRPVs. We are looking forward to seeing how the currents of TRPV and other channels are affected by His-ACBD3, which is supplied via the patch-pipette perfusion of the cytosol.

Reference:

1. Kopperud, R., et al., *cAMP effector mechanisms. Novel twists for an "old" signaling system.* FEBS Letters, 2003. 546(1): p. 121-126.
2. Tasken, K. and E.M. Aandahl, *Localized Effects of cAMP Mediated by Distinct Routes of Protein Kinase A.* Physiol. Rev., 2004. 84(1): p. 137-167.
3. Alto, N., et al., *Intracellular Targeting of Protein Kinases and Phosphatases.* Diabetes, 2002. 51(90003): p. S385-388.
4. Diviani, D. and J.D. Scott, *AKAP signaling complexes at the cytoskeleton.* J Cell Sci, 2001. 114(8): p. 1431-1437.
5. Higashida, H., et al., *Protein kinase C bound with A-kinase anchoring protein is involved in muscarinic receptor-activated modulation of M-type KCNQ potassium channels.* Neuroscience Research, 2005. 51(3): p. 231-234.
6. Rich, T.C. and J.W. Karpen, *Review Article: Cyclic AMP Sensors in Living Cells: What Signals Can They Actually Measure?* Annals of Biomedical Engineering, 2002. 30(8): p. 1088-1099.
7. Taylor, S.S., J.A. Buechler, and W. Yonemoto, *Camp-Dependent Protein Kinase: Framework for a Diverse Family of Regulatory Enzymes.* Annual Review of Biochemistry, 1990. 59(1): p. 971-1005.
8. Pawson, T., M. Raina, and P. Nash, *Interaction domains: from simple binding events to complex cellular behavior.* FEBS Letters, 2002. 513(1): p. 2-10.
9. Tucker, C.L., J.F. Gera, and P. Uetz, *Towards an understanding of complex protein networks.* Trends in Cell Biology, 2001. 11(3): p. 102-106.
10. Lawrence, D.S., *Signaling protein inhibitors via the combinatorial modification of peptide scaffolds.* Biochimica et Biophysica Acta (BBA) - Proteins & Proteomics, 2005. 1754(1-2): p. 50-57.
11. Carnegie, G.K., et al., *AKAP-Lbc Nucleates a Protein Kinase D Activation Scaffold.* Molecular Cell, 2004. 15(6): p. 889-899.
12. Colledge, M. and J.D. Scott, *AKAPs: from structure to function.* Trends in Cell Biology, 1999. 9(6): p. 216-221.
13. Dell'Acqua, M.L., et al., *Regulation of neuronal PKA signaling through AKAP targeting dynamics.* European Journal of Cell Biology. In Press, Corrected Proof.
14. Dell'Acqua, M.L. and J.D. Scott, *Protein Kinase A Anchoring.* J. Biol. Chem., 1997. 272(20): p. 12881-12884.
15. Lohmann SM, D.P., Einig I, Walter U., *High-affinity binding of the regulatory subunit (RII) of cAMP-dependent protein kinase to microtubule-associated and other cellular proteins.* Proc Natl Acad Sci U S A, 1984. 81(21): p. 6723-6727.
16. Burns, L.L., et al., *Isoform Specific Differences in Binding of a Dual-Specificity A-Kinase Anchoring Protein to Type I and Type II Regulatory Subunits of PKA.* Biochemistry, 2003. 42(19): p. 5754-5763.
17. Carr, D.W., et al., *Association of the type II cAMP-dependent protein kinase with a human thyroid RII-anchoring protein. Cloning and characterization of the RII-binding domain.* J. Biol. Chem., 1992. 267(19): p. 13376-13382.

18. Carr, D.W., et al., *Interaction of the regulatory subunit (RII) of cAMP-dependent protein kinase with RII-anchoring proteins occurs through an amphipathic helix binding motif.* J. Biol. Chem., 1991. 266(22): p. 14188-14192.
19. Huang, L.J.-s., et al., *D-AKAP2, a novel protein kinase A anchoring protein with a putative RGS_omain.* PNAS, 1997. 94(21): p. 11184-11189.
20. Burns-Hamuro, L.L., et al., *Distinct interaction modes of an AKAP bound to two regulatory subunit isoforms of protein kinase A revealed by amide hydrogen/deuterium exchange.* Protein Sci, 2005. 14(12): p. 2982-2992.
21. Diviani, D., L. Baisamy, and A. Appert-Collin, *AKAP-Lbc: A molecular scaffold for the integration of cyclic AMP and Rho transduction pathways.* European Journal of Cell Biology. In Press, Corrected Proof.
22. Carr, D.W., et al., *Localization of the cAMP-dependent protein kinase to the postsynaptic densities by A-kinase anchoring proteins. Characterization of AKAP 79.* J. Biol. Chem., 1992. 267(24): p. 16816-16823.
23. Li, H., et al., *Identification, Localization, and Function in Steroidogenesis of PAP7: A Peripheral-Type Benzodiazepine Receptor- and PKA (RI{alpha})-Associated Protein.* Mol Endocrinol, 2001. 15(12): p. 2211-2228.
24. Liu, J., et al., *Molecular cloning, genomic organization, chromosomal mapping and subcellular localization of mouse PAP7: a PBR and PKA-RI [alpha] associated protein.* Gene, 2003. 308: p. 1-10.
25. Liu, J., H. Li, and V. Papadopoulos, *PAP7, a PBR/PKA-RI [alpha]-associated protein: a new element in the relay of the hormonal induction of steroidogenesis.* The Journal of Steroid Biochemistry and Molecular Biology, 2003. 85(2-5): p. 275-283.
26. Tominaga, M., M. Wada, and M. Masu, *From the Cover: Potentiation of capsaicin receptor activity by metabotropic ATP receptors as a possible mechanism for ATP-evoked pain and hyperalgesia.* PNAS, 2001. 98(12): p. 6951-6956.
27. Davis, J.B., et al., *Vanilloid receptor-1 is essential for inflammatory thermal hyperalgesia.* Nature, 2000. 405(6783): p. 183-187.
28. De Petrocellis, L., et al., *The vanilloid receptor (VR1)-mediated effects of anandamide are potently enhanced by the cAMP-dependent protein kinase.* Journal of Neurochemistry, 2001. 77(6): p. 1660-1663.
29. Rathee, P.K., et al., *PKA/AKAP/VR-1 Module: A Common Link of Gs-Mediated Signaling to Thermal Hyperalgesia.* J. Neurosci., 2002. 22(11): p. 4740-4745.
30. Stokes, A.J., et al., *A TRPV2-PKA Signaling Module for Transduction of Physical Stimuli in Mast Cells.* J. Exp. Med., 2004. 200(2): p. 137-147.
31. Smith DB, J.K., *Single-step purification of polypeptides expressed in Escherichia coli as fusions with glutathione S-transferase.* Gene, 1988. 15(67): p. 31-40.
32. di Guan C, L.P., Riggs PD, Inouye H., *Vectors that facilitate the expression and purification of foreign peptides in Escherichia coli by fusion to maltose-binding protein.* Gene, 1988. 15(67): p. 21-30.
33. Gentz R, C.C., Rosen CA, *Bioassay for trans-activation using purified human immunodeficiency virus tat-encoded protein: trans-activation requires mRNA synthesis.* Proc Natl Acad Sci U S A., 1989. 86(3): p. 821-824.
34. Cantrell, A.R., et al., *Molecular Mechanism of Convergent Regulation of Brain Na+ Channels by Protein Kinase C and Protein Kinase A Anchored to AKAP-15.* Molecular and Cellular Neuroscience, 2002. 21(1): p. 63-80.

35. Chen, L., J. Kurokawa, and R.S. Kass, *Phosphorylation of the A-kinase-anchoring Protein Yotiao Contributes to Protein Kinase A Regulation of a Heart Potassium Channel.* J. Biol. Chem., 2005. 280(36): p. 31347-31352.
36. Davare, M.A., et al., *The A-kinase Anchor Protein MAP2B and cAMP-dependent Protein Kinase Are Associated with Class C L-type Calcium Channels in Neurons.* J. Biol. Chem., 1999. 274(42): p. 30280-30287.
37. Mignen, O., J.L. Thompson, and T.J. Shuttleworth, *Arachidonate-regulated Ca2+-selective (ARC) channel activity is modulated by phosphorylation and involves an A-kinase anchoring protein.* The Journal of Physiology, 2005. 567(3): p. 787-798.